Egyptian Journal of Aquatic Biology and Fisheries
Zoology Department, Faculty of Science,
Ain Shams University, Cairo, Egypt.
ISSN 1110 – 6131
Vol. 29(5): 3451 – 3480 (2025)
www.ejabf.journals.ekb.eg

Crayfish as Bioindicators of Heavy Metal Pollution in Egyptian Waters: A Study on Bioaccumulation, Metallothionein Induction, and Human Health Risk Assessment

Abd El-Baset Eladl[1], Mohsen S. Hussein[1], Ahmed Mamoon[1], Mahmoud M. Elsadek[1*], Walid Aly[2], Fawzia S. Ali[2]**
[1] Fish Production Department, Faculty of Agriculture, Al-Azhar University, Cairo, 11884, Egypt.
[2] National Institute of Oceanography and Fisheries (NIOF), Cairo, 11516, Egypt.
***, **Corresponding authors:** md_elsadek@azhar.edu.eg; Fawzias.ali84@gmail.com

ARTICLE INFO

Article History:
Received: July 25, 2025
Accepted: Oct. 3, 2025
Online: Oct. 31, 2025

Keywords:
Procambarus clarkii,
Heavy metals bioaccumulation,
Metallothionein,
Environmental matrices,
Egyptian aquatic ecosystems,
Principal component analysis,
Sediment- water partitioning

ABSTRACT

This research explored the heavy metal distribution patterns that were found in environmental matrices of Egyptian aquatic ecosystems. The study addressed sediment, water, and crayfish tissues from three geographically diverse locations: Kafr El-Sheikh, El-Sharqia, and Mostorod. Seven heavy metals: copper, zinc, cadmium, lead, manganese, iron, and nickel were analyzed to reveal bioaccumulation patterns, matrix-specific distribution, and ecological risk assessment. The result of the principal component analysis showed that the characteristics of the environmental matrix were markedly the major factors that influenced heavy metal distribution, while the first two components accounted for 95.8% of the total variance. In all cases, sediments exhibited the highest concentrations of metals, especially copper (0.500- 0.813mg/ kg) and zinc (0.800- 1.200mg/ kg). Consequently, the role of these sediments as the main sinks in aquatic geochemical cycles was validated. The sediment-to-water partitioning coefficients were larger than 10:1 for most metals, with copper reaching 30:1-45:1, thus the affinity for the solid phases was quite strong. Crayfish (*Procambarus clarkii*) showed remarkable bioaccumulation properties, as cadmium concentrations in their tissues were 13-205 times higher than those in water, hence, they are a species that can particularly accumulate metals in their cells. Concentrations in the water column were low at all sites and manganese (0.011-0.038 mg/kg) and zinc (0.030-0.072 mg/kg) were the most dissolved elements. Bioaccumulation factors differed substantially between locations, and Kafr El-Sheikh showed high values of Cd, Cu, and Mn accumulation. In the same trend, when using metallothionein (MT) analysis, the highest concentrations of MT were recorded in the Kafr El-Sheikh area, which supports the effectiveness of using this technique in detecting pollutants. Health risk assessment showed that the metal consumption amounts are within safe limits for human consumption. The results of the present study offer significant clues about environmental monitoring strategies and pollution control measures in Egyptian freshwater ecosystems.

INTRODUCTION

Heavy metal pollution is a rapidly escalating global crisis. Despite advances in waste management, these non-biodegradable pollutants pose a severe threat to both human and ecological health. Unlike other pollutants, metals persist in the environment **(Velusamy *et al.*, 2022)**. Their increased release into aquatic systems causes significant pollution due to their toxicity, persistence, and ability to bioaccumulate within food chains **(Ali *et al.,* 2019)**. Maintaining suitable freshwater quality is essential for both aquatic and terrestrial life. Monitoring based on relevant bioindicators provides useful data for evaluation of environmental status **(Kumari & Paul, 2020)**. Although the hazards of water contamination by heavy metals are well known, it remains an issue due to expanding industrial development, including mining activities **(Sankhla *et al.,* 2016)**. Macroinvertebrates are frequently suggested as bioindicators for monitoring changing water conditions in areas of potential contamination **(Sumudumali & Jayawardana, 2021)**. In practice, crayfish are of particular importance for biomonitoring studies **(Mathers *et al.,* 2016)**, being the keystone species in most ecosystems in which they occur and, most importantly, can tolerate polluted environments and reflect pollution levels due to accumulation of respective elements in their tissues. While crayfish are useful as bioindicators of contamination, they are also a valuable food source **(Kuklina *et al.,* 2013)**, making monitoring of organ tissue metal concentrations relevant to both animal and human health. The freshwater crayfish, *Procambarus clarkii*, is a North American species introduced to Southeast Asia and other regions in the 1930s. Its rapid growth, ease of management, and high yield make it a promising aquaculture candidate. However, it has also been introduced to the Nile River in Egypt, where it has spread widely throughout the river system and its tributaries **(Aly *et al.,* 2020)**. Furthermore, *P. clarkii* is a valuable food source, with its edible abdominal muscles constituting 10-40% of its total body weight, depending on size and maturity. These muscles are rich in protein, with values reaching 58.6g/ 100g for females and 62.6g/ 100g for males (dry weight basis), and high levels of essential amino acids (EAAs) **(Farrag *et al.,* 2022)**. Therefore, *P. clarkii* can be considered a new, affordable food source that is increasingly popular in Egypt and other countries **(Ibironke *et al.,* 2018)**. Additionally, crayfish are a significant source of polyunsaturated fatty acids (PUFAs) **(Harlıoğlu *et al.,* 2015)** and rich in minerals **(Zhang *et al.,* 2023)**. Egypt's annual crayfish yield is estimated to be around 4.6 tons **(Aly *et al.,* 2020)**. Notably, *Procambarus clarkii* populations can thrive in arid environments, as evidenced by their presence in Egypt's Sinai Desert, facilitated by irrigation networks extending from Giza to Qena governorates **(Farrag *et al.,* 2022)**. While concerns exist about their potential impact on small aquatic organisms and heavy metal accumulation, crayfish play a beneficial role in controlling diseases like schistosomiasis and fascioliasis by feeding on their intermediate host snails **(Mazza *et al.,* 2014)**. Metallothioneins (MTs) are small, heat-resistant proteins rich in cysteine, lacking aromatic amino acids. They can be used as biomarkers to detect metal stress in invertebrates. Crustacean MTs are similar to vertebrate MTs in terms of molecular weight, UV absorption, isoelectric point, and amino acid composition **(Mona *et al.,* 2023)**. Metallothioneins (MTs) play a crucial role in cellular health. They store essential metals like zinc and copper, which are vital for creating metalloenzymes that maintain cellular balance. Additionally, MTs protect cells by binding to harmful non-essential metals such as cadmium, mercury, and silver, reducing their toxic effects **(Labuschagne, 2019)**. This study aimed to compare heavy metal concentrations in crayfish tissues, sediment, and water of three sites in the Egyptian Delta, determine the bioaccumulation and bio sedimentation factors of heavy metals, use metallothionein as an indicator of contamination, and evaluate the possible human health hazards associated with ingestion of crayfish.

MATERIALS AND METHODS

1. The study area

1.1 Mostorod site

Samples were collected from Ismailia Canal (Fig. 1). The Ismailia Canal is a waterway that runs about 125km eastward from the River Nile at Shupra (north of Cairo) to Ismailia City on the Suez Canal. It is the main freshwater source for most of the 12 million inhabitants of the governorates located in the area. The canal has become a source of pollution of various types **(Ramadan *et al.*, 2021)**. The upper section (Cairo to Abu-Zaabal), which is home to the largest industrial zones in Egypt, is the source of pollution from untreated chemical leakages and the presence of heavy metals (especially Fe, Pb, Zn, As, Cd) that come from the factories in the sectors of Shupra El-Kheima, Mostorod, and Abu-Zaabal **(Ibrahim *et al.*, 2014; Hamed, 2019)**. In addition, the agricultural drain, part of the lower section, is working as a source of pollution since it releases waste during the winter coming from the septic tanks, the agricultural effluents, and the municipal discharge. This leads to a rise of the organic matter, the nutrients, and the bacteria as well (up to 390 MPN/ml coliform) **(Ibrahim *et al.*, 2014)**. Additionally, the trihalomethane produced during chlorination treatment will also elevate **(El-Said Salem *et al.*, 2024)**. The canal is providing water for drinking, irrigation, and industrial use to multiple governorates of northern Cairo areas, then continuing through Ismailia Governorate (53 km within borders), with branches extending to Port Said Governorate and Suez Governorate, which irrigate approximately 349,440 hectares and support the major urban centers including Mattaria, Abu-Zaabal, Belbeis, Zagazeeg, and cities along the Suez Canal **(Geriesh *et al.*, 2008; Ramadan *et al.*, 2021)**.

1.2 El- Sharqia site

The samples were collected from El-Salam Canal (Fig. 1). The El-Salam Canal which is the main part of Egypt's Sinai Project has a length of 252.75km—89.75km west of the Suez Canal and 163km beneath it to the east—carrying a 1:1 mixture of Damietta (Nile) freshwater (≈ 2.11 billion m^3/year) and agricultural drainage water (≈ 2.34 billion m^3/year from Bahr Hadous and El-Serw drains), thus elevating salinity, nutrient loads, BOD, pesticide residues, microbial counts, and heavy metals (Fe, Zn, Mn, Pb, Cu, Cd, Cr, Ni) **(Khalifa, 2014; Geriesh *et al.*, 2015; Khalifa, 2020)**. It irrigates the west of Suez the Damietta, Dakahlia, Sharkia, and Port Said governorates while the east of Suez is provided with reclamation and irrigation of 400,000 feddans in North Sinai Governorate's Sahl El-Tina, Raba'a, Bir al-Abd, and southeastern Qantara zones **(Geriesh *et al.*, 2015; Khalifa, 2020; El-Amier *et al.*, 2021)**.

1.3 Kafr El-Sheikh site

At this site we collected the samples from Kitchener Drain (Fig. 1). The Kitchener Drain is Egypt's longest agricultural drainage system which traverses 69 kilometers in the Nile Delta through three governorates (Gharbia, Dakahlia, and Kafr El-Sheikh) before entering the Mediterranean Sea at Baltim City. This crucial waterway is the main source of life for over 11 million people in 182 villages, delivering irrigation water to about 460,000 feddans of agricultural land and at the same time being one of the dirtiest drainage systems in Egypt **(Abd-Elfattah *et al.*, 2021)**. The drain is the recipient of contamination from a wide variety of sources. It receives 75% agricultural drainage water, 23% domestic wastewater, and 2% industrial wastewater; therefore, it is heavily containated with heavy metals (lead, cadmium, zinc, chromium) and pesticides (organochlorine and organophosphorus compounds) in addition to being subject to bacterial contamination estimated beyond the WHO limit resulting from insufficient waste management **(Abd-Elfattah *et al.*, 2021; El-Amier *et al.*, 2023; Metwally *et al.*, 2023)**. The Egyptian government, alongside international organizations (EIB, EBRD, EU), has launched a collaborative comprehensive €481 million depollution project that includes plans for the reconstruction of wastewater treatment plants, implementation of solid waste management systems, and dealing with drainage infrastructure issues, exerting joint efforts to obtain a pollution-free drain with an efficiency for flood control, agricultural irrigation, and aquaculture support **(EBRD, 2018; El-Amier *et al.*, 2023)**.

2. Sampling collection and preparation

To ensure temporal consistency, three replicates for each site were collected during the same sampling period (May 2024). In order to avoid contamination, sampling was achieved with the use of sterilized techniques and acid-washed equipments.

2.1 Estimation of heavy metals in water samples

Samples of water were collected from the three study sites 30cm under the water surface with 1-L pre-cleaned polyethylene bottles (soaked in 10% HNO_3 for 24 h and rinsed with deionized water). To avoid microbial activity and metal precipitation, the samples were acidified with 5mL of concentrated HCl (≥37%, trace metal grade, Merck) for $pH < 2$; this was done immediately after the samples were taken. Samples were stored in an icebox at 4°C and transported to the laboratory within 6 hours of collection. The water sample digestion was carried out using a modified version of the Environmental Protection Agency (EPA) Method 3005A procedures **(EPA, 1992)**. A 500.0mL sample of acidified water was taken in a clean 1000mL beaker to the laboratory. The process was to prepare the acidified water by mixing 20mL of concentrated nitric acid (≥65%, trace metal grade, Merck) and 5.0mL of concentrated sulfuric acid (≥95%, trace metal grade, Merck) in a 4:1 ratio. The mixture was then put on a hot plate and heated at 95°C until the volume was about 10mL, which was the indication of complete digestion (white fumes release). The digest was quantitatively transferred to a 50mL volumetric flask after cooling and was further diluted to volume with ultrapure deionized water (Milli-Q, 18.2 MΩ·cm).

2.2 Estimation of heavy metals in Sediment samples

Sediment samples were collected from the bottom of the same sites using an Ekman-Grab sampler (15 × 15 cm). Samples were immediately transferred to pre-cleaned polyethylene bags, labeled, and stored on ice for transport to the laboratory. Sediment samples were freeze-dried at -80°C for 48 hours and passed through a 1mm clean plastic sieve to remove shell fragments and debris. Sieved sediments were ground in an agate mortar to ensure homogeneity. The powdered sediments were then passed through a clean nylon membrane sieve (0.071mm) and shaken to obtain a fine homogeneous powder. Sediment digestion followed EPA Method 3052 **(Remeteiová *et al.*, 2020)**, with modifications. Approximately 0.5g of dried sediment material was accurately weighed and transferred to acid-cleaned Teflon vessels. Samples were microwave-digested using a MARS 6 microwave digestion system (CEM Corporation) in vessels containing 5mL of ultra-pure nitric acid (≥65%, trace metal grade) and 2mL of ultra-pure concentrated hydrofluoric acid (≥40%, trace metal grade). The microwave digestion program consisted of: Ramping to 200°C over 15 minutes, holding at 200°C for 30 minutes, then, cooling for at least 1 hour. After cooling, vessels were opened and 0.9g of boric acid was added to dissolve fluoride precipitates. Vessels were resealed and placed back in the microwave system for an additional 20 minutes at 150°C. Following cooling for at least 1 hour, the digested sample was quantitatively transferred to a graduated plastic test tube with an additional 0.5mL HF and brought to volume (50mL) with Milli-Q water.

3. Samples and estimation of heavy metal bioaccumulation in crayfish tissues

Crayfish (*Procambarus clarkii*) samples were collected from the same three sites using trammel nets and extended nets. At least 30 individuals were collected from each site (≥ 10 individuals per replicate) and carapace length was kept within 35-45 mm to reduce the effect of size-related variability in metal concentrations. The organisms were sampled and then allowed to cool in order to maintain freshness. Cooling of the samples was done by placing them on ice and transporting them to the lab within 4 hours. To prepare the crayfish samples, they were washed with tap water and then rinsed with deionized water. The samples were dissected in a clean laboratory environment to collect the muscle tissue, gills, and hepatopancreas. The tissues were dried in an oven at 105°C until the weight did not change (usually 24 to 48 hours). The dried tissues were pulverized to a fine powder with a specially cleaned with acid an agate mortar and pestle. Tissue digestion followed EPA Method 3050B **(Edgell, 1996)**, with modifications. Firstly, 2.0g of crushed crayfish tissue was weighed precisely and then transferred to acid-cleaned glass beakers. To digest the samples, 8mL of concentrated nitric acid (≥65%, trace metal grade) was used, and they were placed on the heated plate at 70°C until NO_2 vapor was visible, which is the indication of the initial digestion phase. After that, 8mL of 10% hydrogen peroxide (H_2O_2, trace metal grade) was added in small portions to avoid a vigorous reaction. Heating was continued until the solution turned clear and colorless. The digest was then allowed to cool to room temperature, filtered through Whatman No. 42 filter paper, and the filtrate was quantitatively transferred to a 50mL volumetric flask and made up to volume with ultrapure water. The solutions were stored in acid-washed amber glass bottles at 4°C until the analysis.

Instrumentation and operating conditions

Heavy metal analysis (Cd, Cu, Fe, Pb, Mn, Zn, and Ni) was performed using a SHIMADZU AA-7000 Atomic Absorption Spectrophotometer equipped with deuterium background correction. The instrument was operated under optimized conditions as detailed in Table (1). Metal concentration was calculated using the following formula:

$$Metal\ concentration = \frac{A \times B}{C}$$

A = concentration reading from atomic absorption (mg/L), B = volume of diluted solution (mL), C = volume of original sample (mL) or weight of sediment/tissue sample (g)

Table 1. Instrumental operating conditions for AAS analysis

Element	Wavelength	Slit Width	Lamp Current	Flame	Detection Limit
Cd	228.8	0.7	4.0	Air-C_2H_2	0.005
Cu	324.8	0.7	4.0	Air-C_2H_2	0.010
Fe	248.3	0.2	5.0	Air-C_2H_2	0.050
Pb	283.3	0.7	5.0	Air-C_2H_2	0.020
Mn	279.5	0.2	5.0	Air-C_2H_2	0.010
Zn	213.9	0.7	5.0	Air-C_2H_2	0.005
Ni	232.0	0.2	4.0	Air-C_2H_2	0.050

1. Bioconcentration factor calculation

The bioaccumulation factor (BAF) was calculated using the following formula **(Abbas *et al.*, 2023)**:

$$BAF = \frac{C - crayfish}{C - water}$$

Where, C-crayfish is the concentration of elements in crayfish tissues (mg/kg) and C-water is the concentration of elements in water (mg/L).

However, the bio-sedimentation factor (BSAF) was calculated using the following formula:

$$BSAF = \frac{C - crayfish}{C - sediment}$$

Where, C-crayfish, the concentration of elements in crayfish tissues (mg/kg), and C-sediment, the concentration of elements in sediments (mg/kg).

2. Health Risk Assessment

The estimated daily intake (EDI) was computed using the formula below in mg^{-1} kg^{-1} day^{-1} units **(Chamannejadian *et al.*, 2013)**:

$$EDI = \frac{CF \times IR \times ER \times EP}{BW \times AT} \times 10^{-3}$$

Where, CF stands for the elements concentration in crayfish muscle (mg/kg); IR is the intake rate of crayfish ingested (kg/day), which in this investigation was 20.1 g/day for adults; ER stands for the exposure rate (365 days/year); EP stands for the exposure time over a lifetime (assumed to be 70 years old); BW stands for body weight, which is 70 kg for adults; AT stands for an average lifetime (70 years, 365 days/year). However, the formula below, which was developed from the ratio of EDI to RfD (oral reference dose), was used to determine target hazard quotient (THQ) as:

$$THQ = \frac{EDI}{Rf\,D}$$

Where, RfD stands for elements oral reference doses (mg/kg/days) according to **The Risk Assessment Information System (2019)**.

Moreover, the hazard index (HI) is a mathematical formula that calculates the non-carcinogenic hazard by summing the THQ values of metals under study **(Antoine *et al.*, 2017)** as follows:

$$HI = \sum_{N=1}^{i} THQ_{n}$$

3. Metallothionein analysis

The spectrophotometric method, as described by **Viarengo *et al.* (1997)** and **UNEP/RAMOGE (1999)**, with a few modifications, was applied to detect MTLPs in crayfish. This method has been reported to be a sensitive, time-saving, and low-cost technique able to detect metallothionein content in the tissues of marine organisms and has been intercalibrated and standardized by a number of laboratories **(UNEP/RAMOGE, 1999; Zorita *et al.*, 2005)**. Three subsamples (in order to minimize experimental errors) of about 1g (washed, wet weight) were accurately weighed from soft tissues belonging to at least ten bivalves and whole tissue of sponges after they were physically homogenized using a pestle and mortar to produce one pool of homogenized tissue per site. Tissue samples were homogenized by homogenizing buffer of 0.5M sucrose, 20mM Tris–HCl (pH 8.6), 0.006mM leupeptin, 0.5 mM PMSF, and 0.01% ß-mercaptoethanol then centrifuged for 30min at 28,600 × g (times gravity) at 4°C. The supernatant solution was purified with 1.05mL cold ethanol (−20°C) and 80µL chloroform (per 1 ml of supernatant) and centrifuged for 10min at 6000 ×gat 4°C. Then 40µL concentrated HCl and three volumes of cold ethanol (−20 °C) allowed the proteins to denature for 1h at−20°C. This was then centrifuged for 10min at 6000 ×g, and the pellet was saved. RNA was not added in the MT precipitation step as this has been shown to be un-necessary **(Viarengo *et al.*, 1997)**. The pellet was then washed with a mixture of the previously described buffer solution (without the ß-mercaptoethanol), cold ethanol and 80µL chloroform and centrifuged for 10min at 6000 ×g. The supernatant was discarded and the pellet was dried with N2gas. The pellet was resuspended with 150µL 0.025 M NaCl and 150µL 1 N HCl with 4 mM EDTA. After resuspension, 4.2mL of a solution containing 2 M NaCl and 0.43 mM DTNB and 0.2 M NaH2PO4(pH 8.0) was added, and centrifuged for 5min at 2500 rpm. The absorbance was read at 412 nm against standard solutions of reduced glutathione (GSH) using a UV–visible spectrophotometer.

4. Statistical analysis

The statistical analysis was carried out using IBM SPSS Statistics Version 22 (SPSS Inc., IL, USA). The Shapiro-Wilk test was used to check data normality. Duncan's multiple range test **(Duncan, 1955)** was used to determine which element levels at different sites were significantly different; when a one-way analysis of variance (ANOVA) test produced significant differences for each element ($P< 0.05$) element levels were further investigated. Principal component analysis (PCA) was employed to investigate statistical relationships between the three locations based on element levels. Pearson and Spearman's rank correlation coefficients between element levels in sediment, water, and crayfish tissues across sites were calculated. All data are presented as mean ± standard error, and statistical significance was set at $P< 0.05$.

RESULTS

1. Heavy metal distribution patterns across the different sites

These data reflect the bioaccumulation of seven heavy metals in three different aquatic environments in Egypt (Table 2). The data show that these metals tend to accumulate in discrete compartments due to significant geographical variability in pollution levels. This study gives evidence for the partitioning of metals by environmental matrices, with sediments always bearing the most metal load for the majority of metals, especially copper (0.500-0.813 mg/kg) and zinc (0.800-1.200 mg/kg), thus confirming their role as the main sinks for heavy metal contamination in the geochemical cycle. Research on bioaccumulation patterns in crayfish demonstrates that these animals have species-specific mechanism for sequestering metals. For instance, cadmium is the metal which varies most greatly in different locations (0.080-0.410 mg/kg), increasing five times from Mostorod to Kafr El-Sheikh, therefore, anthropogenic activities are the probable sources of pollution in the two areas. The bioaccumulation factors illustrate that crayfish have the capability to choose the metals that they will accumulate the most, with cadmium concentrations in crayfish tissue being 13-205 times higher than corresponding water concentrations, besides, they maintain relatively lower levels for other metals, hence, these processes of biological regulation and detoxification are active. The level of metals in the water column remains low at each site; manganese (0.011-0.038 mg/kg) and zinc (0.030-0.072 mg/kg) are the metals with the highest dissolved fractions. The sediment-to-water partitioning coefficients of most metals are greater than 10:1, which is especially evident for copper (30:1-45:1), indicating that copper has a high affinity for sorption and also that sediment is the major reservoir compartment of these aquatic systems. Nickel was not found in any of these matrices in any location. Nickel concentrations are either below detection limits, or the metal is environmentally excluded. The patterns of statistical significance (indicated by letter designations) reveal that limited places have an influential role in metal-dependent deposition in sediments and biota; however, the deposition in the water column shows no significant differences between locations.

A. Heavy metal concentrations in environmental samples

This principal component analysis biplot (Fig. 2) shows heavy metal pollution that has been distributed in sediments, water, and crayfish specimens from three Egyptian places: Kafr El-Sheikh, El-Sharqia, and Mostorod. This PCA also illustrates that the environmental matrix type, and not the location, is the key factor determining the metal distribution that goes across the places. The first two components account for 95.8% of the total variance (PC1: 64.2%, PC2: 31.6%); thus, these directions efficiently grab the major heavy metal contamination patterns. The sample points are gathered differently by matrix types: sediments are in the upper region, water samples are in the lower right quadrant, and crayfish are on the left side of the plot. The loading vectors indicate that lead (Pb) and manganese (Mn) are the most influential drivers of difference, as the direction of their arrows is toward the upper right quadrant, where sediment samples are located. The vectors of zinc (Zn) and iron (Fe) point to the upper left, whereas cadmium (Cd) is the least contributor to variance. The pollution sources are different for each matrix; this is indicated by the clear matrix-based clustering: sediments become heavy metals storage for a long time, water samples are more mobile contamination fractions, and crayfish represent biological uptake patterns that are entirely apart from environmental concentrations. Such a gap, therefore, gives an indication that bioaccumulation processes in aquatic organisms take different routes than just simple environmental exposure. The spatial pattern shows that apart from distance, the same basic processes govern heavy metal distribution in all three locations and across environmental compartments. This pattern endorses the use of matrix-specific monitoring approaches instead of location-based strategies for environmental assessment.

B. Correlation analysis of heavy metal concentrations across sites and sample types

The Pearson correlation heat map (Fig. 3) shows that heavy metals have different co-occurrence patterns in three places, where samples were taken, and in different sample matrices. Among the crayfish samples obtained from different places, there were very strong positive correlations ($r > 0.9$), with Mostorod_crayfish vs El-Sharqia crayfish having the highest correlation of $r = 0.99$, representing the same bioaccumulation patterns in all the locations. Consequently, sediment samples also had great inter-site correlations ($r= 0.78-1.0$) and were indicative of uniform sediment contamination processes for the region. In addition, water samples had moderate to strong correlations between sites ($r= 0.57-0.93$). In particular, El-Sharqia_water was very strongly correlated with other sample types (r = 0.71-0.89). The correlation matrix indicated quite clearly that sample type was more of a deciding factor of metal concentration patterns than the geographical location of the sampling site, this being illustrated by stronger correlations among similar matrices in different locations than among different matrices in the same place. The weakest correlations were found between Mostorod water and the other sediment samples (r = 0.37-0.41) and this most probably reflects geochemical or hydrological processes, which are specific to that place. These correlation patterns express that they are coming from common pollution sources and that these heavy metals have similar environmental transport and fate processes within the aquatic ecosystem that was investigated, with bioaccumulation in crayfish showing the most consistent behavior at all three sites.

C. Site-specific heavy metal correlations using spearman rank analysis

The site-specific correlation analysis charts the specific interrelations between heavy metals at each sampling spot with the use of Spearman's rank correlation coefficient (Fig. 4). The Mostorod site is characterized by very strong correlations among metal pairs, with Fe-Mn (*P*= 1.0), Cu-Fe (*P*= 0.87), and Cd-Cu (*P*= 0.87) being the most significant. This means that the site is probably contaminated with metals of the same source or that their environmental behavior at the site is similar. El-Sharqia site is also characterized by another correlation structure which is composed of very strong ones, such as Cu-Mn (*P*= 1.0), as well as some moderate to strong among Cd, Fe, and Pb (*P*= 0.5 to 0.87). What is interesting and deserves our attention is that the site shows some negative correlations, especially Ni with other metals (*P*= -0.5 to -0.87), and this may signify that the sources of the metals are not the same or that environmental processes are acting in opposition. The most complex correlation structure is found at Kafr El-Sheikh where there are not only strong positive correlations but also negative ones, for example, Mn-Pb (*P*= 1.0), Fe-Pb (*P*= 1.0), Fe-Mn (*P*= 1.0), and negative correlations corresponding to Cd with several metals. Thus, the differences among these correlation structures indicate that local environmental factors are the major driving force influencing the behavior of heavy metals. This means that each site is going to be affected by different pollution sources or by different geochemical conditions in the different sites.

E. Biota accumulation factor (BAF) concentrations

The bioaccumulation factor results are presented in Table (3). The results showed significant increase of BAF of CD, Cu and Mn in Kafr El-Sheikh site compared to other sites. In contrast, The BAF of Fe showed increasing significant in Mostorod site compared to other sites. However, Mn and Cu showed lowest values compared to other heavy metals.

F. Biota–sediment accumulation factor (BSAF)

The results of Biota–sediment accumulation factor are presented in Table (4). Kafr El-Sheikh site showed significant increase in all heavy metals were measured in this study compared to El-Sharqia and Mostorod sites. However, Cd showed the highest values at all sites compared to other heavy metals.

G. Health risk parameters

Estimated daily intakes (EDI), target hazard quotients (THQ) and hazard index (HI) of heavy metals through the consumption of fish in the present study are presented in Table (5). In the current study, the highest EDI was found as Zn. This was followed by Cd, Fe, and Cu. However, Kafr El-Sheikh site showed the highest values of EDI compared to other sites. THQ was calculated for each metal on the basis of the oral reference dose; there was no apparent risk when each metal was analyzed individually. Its sum (HI) was also found to be less than 1, which means that consuming fish is not harmful to human health.

H. The comparison between heavy metals in sites and the standard percentage

Fig. (5) elucidates the juxtaposition of the conventional risk assessment pertaining to heavy metals alongside the concentrations of heavy metals present in the tissues of crayfish. The findings suggest a notable elevation in the concentrations of Cd and Zn within the crayfish tissues when juxtaposed with the established target risk thresholds across all sampling locations; nonetheless, these concentrations remain within an acceptable range for human consumption, as delineated by the Estimated Daily Intake (EDI) value. Conversely, Cu and Fe exhibited comparatively minimal concentrations relative to the risk assessment benchmarks across all locations.

I. The percentage contribution of heavy metals to the hazard index

The findings are illustrated in Fig. (6), which delineates the percentage contributions of heavy metals to the hazard index (HI) across all sampling sites. The cadmium (Cd) element exhibited the highest contribution percentage in comparison to all other elements across the various sites, followed by zinc (Zn), copper (Cu), and iron (Fe), respectively. Notably, Kafr El-Sheikh recorded the most significant percentage contribution of Cd, whereas El-Sharqia demonstrated the highest percentage contribution of Zn in relation to other locations.

J. Metallothionein concentration

The results of metallothionein protein showed increasing in muscle tissue compared to gills and hepatopancreas. In contrast, the Kafr El-Sheikh site showed increasing of metallothionein protein in all organs compared to El-Sharqia and Mostorod sites, except hepatopancreas in Mostorod (Fig. 7).

DISCUSSION

The results of this study show that preferential accumulation of heavy metals in sediments rather than water columns is extensively documented and represents a major characteristic of metal fate in aquatic ecosystems. The metal content is predominantly associated with sediment, where the concentration of copper (0.500-0.813 mg/kg) and zinc (0.800-1.200 mg/kg) are particularly high. Such concentrations indicate the modifying effect of multiple concurrent physicochemical processes on metal distribution **(Adekolurejo *et al.*, 2023; Dhiman *et al.*, 2023; Gupta *et al.*, 2025)**. Sediments act as the main sink of metal pollution due to their large surface area and abundance of active binding sites that enable metal uptake through adsorption, co-precipitation, and incorporation into mineral matrices **(Lim *et al.*, 2012; Dhiman *et al.*, 2023; Li *et al.*, 2025)**. The sequestration of metals observed is consistent with the basic geochemical principles, which describe the role of particulate matter in suspension as a very efficient scavenging mechanism for dissolved metals **(Lim *et al.,* 2012; Dhiman *et al.,* 2023)**. Studies from the Ganga River basin demonstrated similar distribution patterns, where suspended particulate matter served as the primary sink for metals, followed by bed sediments **(Dhiman *et al.,* 2023)**. This sequential metal partitioning occurs because fine particles possess greater specific surface areas and enhanced metal-binding capacity compared to larger sediment fractions **(Rendina *et al.,* 2001; Das *et al.,* 2015)**.

The sediment-focused distribution pattern is indicative of various issues including long-term metal cycling and ecosystem health. Sediments have the potential of being either sinks or sources; however, this is highly dependent on the changing environmental conditions such as pH, redox potential, and the content of organic matter **(Hacısalihoğlu & Karaer, 2016; Gupta *et al.,* 2025; Kutlu *et al.,* 2025)**. The mobility of metals under anoxic conditions could be enhanced by the reductive dissolution process which may lead to the release of metals, initially captured being returned to the water phase **(Das *et al.*, 2015; Hacısalihoğlu & Karaer, 2016)**.

The remarkable bioaccumulation capacity observed in crayfish tissues, particularly the 13- 205-fold concentration factor for cadmium relative to water concentrations, demonstrates the complex biological processes governing metal uptake in freshwater crustaceans **(Stanek *et al.,* 2014; Abbas *et al.,* 2023)**.

This bioconcentration is very peculiar because of special physiological mechanisms that crayfish have for metal handling, like selective uptake, tissue-specific distribution, and detoxification processes **(Stanek *et al.,* 2014; Abbas *et al.,* 2023)**. The hepatopancreas is the main place where metals gather in crayfish, and it is thus a digestive and detoxification organ **(Stanek *et al.,* 2014)**. In this place, the metals are stored in crayfish tissues after the order: hepatopancreas > exoskeleton > digestive tract > abdominal muscle, with zinc as the element that was present in the highest concentrations in muscle tissue **(Stanek *et al.,* 2014)**. This organ-specific distribution constitutes the biological regulation mechanisms through which crayfish deal with metal exposure and at the same time they manage their physiological functions without any problem. The fact that this is a species-specific characteristic of metal bioaccumulation is due to the physiological adaptations being different, and also the ecological niches, and feeding behaviors of the animals **(Abbas *et al.,* 2023; Jibrin *et al.,* 2025)**. The shell of the crayfish is the main area where the metal is greatly absorbed because the chitin that it is made of, which has functional groups such as amines and hydroxyls that help the metal-binding process **(Stanek *et al.,* 2014)**. However, the bioaccumulation patterns among various metals can be highly different as essential elements like copper and zinc are distributed in different areas compared to non-essential toxic metals like cadmium **(Stanek *et al.,* 2014; Abbas *et al.,* 2023)**. The five-fold increase in cadmium concentrations from Mostorod to Kafr El-Sheikh provides compelling evidence for anthropogenic pollution sources affecting aquatic metal distribution **(Cheng *et al.,* 2015; Hussain *et al.,* 2022; Vallese *et al.,* 2025)**. Such spatial variability emphasizes the uneven distribution of pollution sources across the Egyptian territory that are probably coming from the industries, agriculture, and urban areas **(Pastor-Arbulú & Rodríguez-Delfín, 2025; Vallese *et al.*, 2025)**. Cadmium sources of anthropogenic nature are largely cited all over the world. The main agents are industrial emissions, fertilizers of phosphate, and the discharge of wastewater **(Chunhabundit, 2016; Peana *et al.*, 2022; Vallese *et al.*, 2025)**. The atmospheric emission inventory from China revealed that cadmium emissions from anthropogenic sources showed gradually ascending trends linked to increased coal consumption and industrial production **(Vallese *et al.*, 2025)**. Similar patterns likely explain the observed gradient in Egyptian aquatic systems, where cumulative inputs from diverse anthropogenic sources create distinct contamination signatures. The exceptional bioaccumulation of cadmium (ranging 13-205 times water concentrations) reflects this element's particular toxicological significance and biogeochemical behavior **(Halim *et al.*, 2021; Vallese *et al.*, 2025)**. Cadmium's tendency to bind strongly to biological tissues, combined with extremely slow elimination rates, results in progressive bioaccumulation that can reach concentrations harmful to both organisms and their predators **(Peana *et al.*, 2022)**. The biological half-life of cadmium in organisms can exceed several years, making it a persistent contaminant of particular concern **(Pastor-Arbulú & Rodríguez-Delfín, 2025)**.

Low dissolved metal concentrations were observed in water columns, which were consistent, particularly for manganese (0.011-0.038 mg/kg) and zinc (0.030-0.072 mg/kg) and reflected the dynamic equilibrium between different environmental compartments and the strong binding of metals to the particulate phases **(Bruland *et al.*, 2006; Butler *et al.*, 2008; Gerringa *et al.*, 2020)**. The distribution pattern of metals is consistent with the principle of metal speciation in aquatic systems, where most of the metals are found in particulate-bound forms rather than dissolved phases **(Bruland *et al.*, 2006; Butler *et al.*, 2008)**. This pattern of metal distribution has been generally reflected in a variety of studies involving different water bodies. The dominance of particulate-associated metals over dissolved forms is a feature that has been observed repeatedly in various aquatic environments. Work in acid mine drainage systems showed that dissolved fractions accounted for more than 90% of manganese, about 75% of zinc, about 30% of copper, and less than 10% of iron on average **(Butler *et al.*, 2008)**. The latter patterns are manifestations of the different metals' varying degrees of affinity for particulate surfaces, and their propensity to undergo hydrolysis and precipitation.

Chemical parameters of water greatly affect the speciation of metals and bioavailability in the dissolved phase **(Bruland *et al.*, 2006; Gerringa *et al.*, 2020)**. Some parameters such as pH, dissolved organic carbon, ionic strength, and competing ions form a complicated system of equilibrium that govern the final place and biological availability of the dissolved metals **(Peters *et al.*, 2024)**. The metal-organic complexation, to be more exact, greatly hampers the metal bioavailability due to it being stabilized and not recognized as bioavailable **(Peters *et al.*, 2024)**.

The observed sediment-to-water partitioning coefficients exceeding 10:1, with copper showing particularly high ratios of 30:1-45:1, demonstrate the exceptional affinity of this metal for solid phases **(Rendina *et al.,* 2001; Jung *et al.,* 2005; Nurdini *et al.,* 2024)**. These partitioning coefficients reflect the combined influence of sorption processes, precipitation reactions, and incorporation into mineral structures **(Rendina *et al.,* 2001; Jung *et al.,* 2005; Das *et al.,* 2015)**. Copper's elevated partitioning coefficient specifically reflects its strong binding affinity for various surface sites, including organic matter, iron and manganese oxides, and clay minerals **(Rendina *et al.,* 2001; Burton *et al.,* 2005)**. The geochemical partitioning of copper has been extensively studied, with research from the Reconquista River revealing that copper was predominantly associated with organic matter and sulfide phases, which are generally more stable under reducing conditions **(Peters *et al.,* 2024)**. The high partitioning coefficients have important implications for metal cycling and long-term fate in aquatic systems. Metals with high solid-water distribution coefficients tend to be less mobile and less bioavailable, but they also represent long-term contamination sources that can be remobilized under changing environmental conditions **(Jung *et al.,* 2005; Nurdini *et al.,* 2024)**. The stability of these metal-sediment associations depends on factors such as pH, redox conditions, and the presence of competing ligands **(Das *et al.*, 2015; Hacısalihoğlu & Karaer, 2016)**. The complete absence of nickel across all environmental matrices and sampling locations raises important questions about environmental exclusion processes and analytical detection capabilities **(B.C. Ministry of Water, 2024; Peters *et al.,* 2024)**. Nickel concentrations below detection limits could reflect either genuine environmental exclusion or limitations in analytical methodology **(Binet *et al.,* 2018; B.C. Ministry of Water, 2024)**.

Typically, nickel's present-day analytical practical quantitation limit falls in the range of 0.03 to 0.5µg/ L with ICP-MS instruments. The practical quantitation limit for nickel is also informally declared as 0.1µg/ L in fresh water **(B.C. Ministry of Water, 2024)**. Freshwater ecosystems have natural nickel concentrations that usually fall within 0.1 to 10µg/ L range, but in places that are naturally rich in nickel, the concentration can go as high as 10,000µg/ L **(B.C. Ministry of Water, 2024)**.

Environmental conditions are the key players that shape nickel's nature and determine its availability to organisms in water bodies. Nickel toxicity decreases with increased water hardness and is weakly complexed by dissolved organic matter, making it less bioavailable when adsorbed to suspended material **(Peters *et al.,* 2024)**. The absence of detectable nickel in the Egyptian systems could reflect strong complexation with organic matter or rapid removal through adsorption processes, particularly if the systems have high organic carbon content or abundant sorption sites **(Binet *et al.,* 2018)**.

The distinct correlation structures observed across the three sampling sites provide valuable insights into metal source origins and environmental processes **(Kamble, 2020; Zaitsev *et al.,* 2020; Du & Lu, 2022)**. The strong positive correlations observed at Mostorod between iron-manganese (P= 1.0), copper-iron (P= 0.87), and cadmium-copper (P= 0.87) suggest common source origins or shared geochemical behavior patterns **(Du & Lu, 2022; Salauddin *et al.,* 2023)**. Perfect or near-perfect correlations between metal pairs often indicate either common anthropogenic sources or coupled geochemical processes **(Zaitsev *et al.*, 2020; Du & Lu, 2022)**. The iron-manganese correlation observed across multiple sites reflects their similar geochemical behavior, as both metals are often co-precipitated under oxidizing conditions and can be simultaneously mobilized under reducing conditions **(Kamble, 2020; Zaitsev *et al.*, 2020)**. Studies from urban topsoil demonstrated that iron and manganese correlations typically indicate natural lithogenic sources, while correlations with other metals suggest anthropogenic inputs **(Du & Lu, 2022)**. The negative correlations observed at El-Sharqia, particularly involving nickel with other metals (P= -0.5 to -0.87), indicate either different source origins or competing environmental processes **(Du & Lu, 2022; Salauddin *et al.*, 2023)**. Negative correlations can arise from several mechanisms, including competitive adsorption for binding sites, different solubility behaviors, or contrasting responses to environmental conditions such as pH or redox changes **(Du & Lu, 2022; Salauddin *et al.*, 2023)**.

The complex correlation structure observed at Kafr El-Sheikh, with strong positive correlations between manganese-lead (P= 1.0), iron-lead (P= 1.0), and iron-manganese (P= 1.0), alongside negative correlations involving cadmium, reveals the site-specific nature of metal behavior and source influences **(Diamantini *et al.*, 2018; Du & Lu, 2022)**. These patterns suggest that local environmental factors exert the greatest influence in determining heavy metal behavior, rather than regional atmospheric deposition **(Du & Lu, 2022)**. The site-specific variation in correlation structures demonstrates that each location is likely impacted by different pollution sources or operates under distinct geochemical conditions **(Diamantini *et al.*, 2018; Du & Lu, 2022)**. Industrial activities, agricultural practices, and urban development create characteristic geochemical fingerprints that manifest as specific metal association patterns **(Du & Lu, 2022; Salauddin *et al.*, 2023)**. The presence of strong positive correlations typically indicates either common sources or similar environmental fate processes, while the absence of correlation or negative relationships suggests independent sources or competing processes. Spearman rank correlation analysis is particularly valuable for environmental assessment because it captures monotonic relationships without assuming linear associations, making it more robust for environmental data that often exhibit non-normal distributions **(Diamantini *et al.*, 2018)**. The correlation patterns observed in this study provide a foundation for source apportionment studies and can guide targeted pollution control strategies by identifying the most likely sources of metal contamination.

The highly elevated biota-sediment accumulation factors noted at Kafr El-Sheikh, where cadmium registered the maximum figures in all the sampling stations, signify that the bioavailability of the metals has been increased and pollution risks are likely elevated **(Thomann *et al.*, 1995; Zahedi, 2018; Melake *et al.*, 2023)**. Biota-sediment accumulation factors (BSAFs) are important indicators for estimating the movement of pollutants from sediments to living tissues and the possibility of their biomagnification in the food chain **(Thomann *et al.*, 1995; Melake *et al.*, 2023)**.

Values of BSAFs exceeding unity suggest that organisms actively concentrate metals from their environment through efficient uptake mechanisms or reduced elimination processes **(Thomann *et al.*, 1995; Melake *et al.*, 2023)**. The exceptional cadmium bioaccumulation observed across all sites reflects this element's particular tendency to accumulate in biological tissues and its slow elimination kinetics **(Melake *et al.*, 2023; Younis *et al.*, 2023)**. Studies from Iranian coastal waters revealed similar patterns, where cadmium consistently showed the highest bioaccumulation factors among various metals studied **(Zahedi, 2018)**. The spatial variation in BSAFs, with Kafr El-Sheikh exhibiting significantly higher values, suggests local phenomena that are conducive to metal bioavailability **(Melake *et al.*, 2023; Younis *et al.*, 2023)**. The most probable sources of these factors are sediment properties, which may be grain size, organic matter content, pH, and the presence of acid-volatile sulfides that can affect the metal speciation and consequently the availability for biological uptake **(Thomann *et al.*, 1995; Melake *et al.*, 2023)**. The higher BSAFs in this location suggest either enhanced metal bioavailability due to favorable geochemical conditions or reduced organism capacity for metal regulation and detoxification.

Results of the research are consistent with typical findings in literature concerning heavy metal bioaccumulation and health risk assessment. Research outcomes show that zinc gave the highest estimated daily intake (EDI) values, after that there was cadmium, iron, and copper; however, the health risk evaluation by total hazard quotient (THQ) and hazard index (HI) methods indicate that consumption of these metals within limits is safe for human health.

The hazard index (HI) staying lower than 1 agrees with a number of international publications that have carried out heavy metal risk assessment in fish consumption. Researches which cover different continents such as Bangladesh, Nigeria, or Mediterranean have also found this that the HI values are still under 1, the safe limit and thus, consumers have no need to worry about the non-carcinogenic risk. It can be concluded that the pollution situation is still at the level that is detectable but not high enough to cause health problems through the consumption of fish in moderate amounts **(Thiep *et al.*, 2020; Mamun *et al.*, 2024)**. The finding that cadmium had the highest percentage contribution in the hazard index is well-known in the toxicological literature. The focus on cadmium in the risk assessment calculations is because it has high toxicity potential and possesses lower reference dose values than the other metals. In this respect, cadmium has been categorized as one of the most dangerous heavy metals (Agency for Toxic Substances and Disease Registry classification) in addition to being the metal that most preferentially bioaccumulates in metabolically active tissues **(Liu *et al.*, 2022; Lee *et al.*, 2024)**. The high level of cadmium in the crayfish tissues, though not exceeding the allowed limit of EDI, needs to be continuously checked. By reviewing the available studies in literature on cadmium bioaccumulation in aquatic organisms, one can infer that during the chronic exposure of specific tissues, an accumulation of substances was detected, specifically in the liver and gills, with values higher than those accumulated in muscle tissue. The bioaccumulation hierarchy generally remains as follows: liver > gills > muscle > other tissues and this is the reason why the muscle tissue (the major user of human consumption) is usually recorded with the lowest level of contamination **(Senarathne & Pathiratne, 2010; Ali *et al.*, 2025)**.

Metallothionein protein concentrations in muscle tissue that have been increased significantly in comparison with gills and hepatopancreas are the main cellular defense mechanism that is fighting heavy metal toxicity. Proteins of metallothionein are primary cellular detoxification agents for heavy metals, such as cadmium, zinc, and copper forming a huge sum of metals. The tissue-specific distribution of metallothionein expression mirrors the physiological demand for metal detoxification in different organs **(Wang *et al.*, 2014; M'Kandawire *et al.*, 2017)**.

The heightened metallothionein levels in Kafr El-Sheikh samples from different tissues imply a response of the biology to increased environmental metal stress here. This reaction map is consistent with metallothionein's function as a quick biomarker for heavy metal pollution, where the quantity of expression follows closely the exposure of metal and time of the experiment. Data from experiments suggest that metallothionein expression is the highest in tissues involved in metal uptake, storage, and excretion, including liver, gills, and kidneys **(Min *et al.*, 2016; M'Kandawire *et al.*, 2017)**. The coexistence of increased cadmium and zinc contents and safe EDI values means that the contamination levels are not far from but still within the limits for consumption. Nevertheless, site differences and the changes in metallothionein make it possible to continue monitoring the environment and controlling sources of pollution **(Páez-Osuna *et al.*, 2023; Almafrachi *et al.*, 2025)**. The preferential accumulation pattern (cadmium > zinc > copper > iron) in hazard index contributions reflects both the relative toxicity of these metals and their environmental availability. This pattern emphasizes the importance of cadmium source reduction and water quality management in aquaculture systems, particularly in high-contamination areas like Kafr El-Sheikh **(Biswas *et al.*, 2023; Mishra *et al.*, 2024; Almafrachi *et al.*, 2025)**.

CONCLUSION

The high concentration of heavy metals in the sediments indicates that these compartments will, in fact, continue to provide metals for the environment for a long time after the input has been stopped, and hence, it is necessary to conduct long-term monitoring and possible active remediation strategies. The species-specific bioaccumulation patterns observed in crayfish clearly indicate that these organisms may be used as bioindicators for ecosystem health assessment, thus they can provide integrated exposure information which can be used for management decisions and for setting up early warning systems for environmental degradation. The metal distribution patterns, and the bioavailability of the metal vary over short distances, and this means that it is necessary to have a very detailed and specific approach for the assessment of each site rather than conducting all the work on large generalization basis. Knowing the particular contributors that influence each site helps us to choose the right management intervention. For example, we can decide to focus on industrial point sources if they are predominating, or on agriculture non-point sources, etc. The comprehensive health risk assessment confirms that heavy metal contamination levels in fish tissues are well below the limits of safety for human food today, with hazard index values below 1, thus no non-carcinogenic health risks either immediate or probable are identified. Therefore, environmental monitoring, together with the regulation of pollution sources, is still necessary in order to prevent the possible growth of contamination in the future and to keep fish safe for consumers. Thus, we believe that, the widely distributed heavy metal patterns and bioconcentration factors presented in this research paper carry weight in environmental stewardship and the evaluation of ecological conditions in the water bodies of Egypt.

Funding Declaration: There is no funding for this research.

REFERENCES

Abbas, M.M.M.; Abd El-Aziz, M.A.E.; Kaddah, M.M.Y.; Hassan, A.K.; El-Naggar, H.A.; Radwan, M.; El-Tabakh, M.A.M.; Afifi, M.A. and Bashar, M.A.E. (2023). Bioaccumulation, Biosedimentation, and Health Hazards of Elements in Crayfish, *Procambarus clarkii* from El-Rahawi Drain and El-Qanatir in the River Nile, Egypt. *Biological Trace Element Research*, *201*, 3050-3059.

Abd-Elfattah, E.A.; Sheta, A.E.A.; Saifeldeen, M.; Hassanein, S.A. and Mahmoud, Y.I. (2021). Assessment of water and sediments quality of Kitchener Drain Nile Delta-Egypt. *Arab Universities Journal of Agricultural Sciences*, *29*, 801-811.

Adekolurejo, O.; Osungbemiro, N.; Adeyem, O. and Falowo, T. (2023). Heavy metal concentrations and distribution in water, sediment, and catfish, *Clarias gariepinus* obtained from aquaculture farms in Ondo, Nigeria. *Science View Journal*, *4*, 279-284.

Ali, H.; Khan, E. and Ilahi, I. (2019). Environmental chemistry and ecotoxicology of hazardous heavy metals: environmental persistence, toxicity, and bioaccumulation. *Journal of Chemistry*, *2019*, 6730305.

Ali, Z.; Sher, N.; Muhammad, I.; Nayab, G.E.; Alouffi, A.; Almutairi, M.M.; Khan, I. and Ali, A. (2025). The combined effect of cadmium and copper induces bioaccumulation, and toxicity and disrupts the antioxidant enzymatic activities of goldfish (*Carassius auratus*). *Toxicology Reports*, *14*, 101972.

Almafrachi, H.A.A.; Gümüş, N.E. and Çorak Öcal, İ. (2025). Heavy metal bioaccumulation in fish: implications for human health risk assessment in ten commercial fish species from Konya, Türkiye. *International Journal of Environmental Science and Technology*, *22*, 4065-4074.

Aly, W.; El-Far, A. and A Fetouh, M. (2020). Some fisheries and biological aspects of the crayfish *Procambarus clarkii* (Girard, 1852) in the River Nile, Egypt. *Egyptian Journal of Aquatic Biology and Fisheries*, *24*, 33-42.

Antoine, J.M.R.; Fung, L.A.H. and Grant, C.N. (2017). Assessment of the potential health risks associated with the aluminium, arsenic, cadmium and lead content in selected fruits and vegetables grown in Jamaica. *Toxicology Reports*, *4*, 181-187.

B.C. Ministry of Water, Land and Resources Stewardship. (2024). *Nickel Water Quality Guideline for the Protection of Freshwater Aquatic Life-Technical Report*. Water Quality Guideline Series.

Binet, M.T.; Adams, M.S.; Gissi, F.; Golding, L.A.; Schlekat, C.E.; Garman, E.R.; Merrington, G. and Stauber, J.L. (2018). Toxicity of nickel to tropical freshwater and sediment biota: A critical literature review and gap analysis. *Environmental Toxicology and Chemistry*, *37*, 293-317.

Biswas, A.; Kanon, K.F.; Rahman, M.A.; Alam, M.S.; Ghosh, S. and Farid, M.A. (2023). Assessment of human health hazard associated with heavy metal accumulation in popular freshwater, coastal and marine fishes from south-west region, Bangladesh. *Heliyon*, *9*, e20514.

Bruland, K.; Middag, R. and Lohan, M. (2006). Controls of trace metals in seawater. *Treatise on Geochemistry*, *6*, 23-47.

Burton, E.D.; Phillips, I.R. and Hawker, D.W. (2005). Geochemical Partitioning of Copper, Lead, and Zinc in Benthic, Estuarine Sediment Profiles. *Journal of Environmental Quality*, *34*, 263-273.

Butler, B.A.; Ranville, J.F. and Ross, P.E. (2008). Observed and modeled seasonal trends in dissolved and particulate Cu, Fe, Mn, and Zn in a mining-impacted stream. *Water Research*, *42*, 3135-3145.

Cheng, K.; Wang, Y.; Tian, H.; Gao, X.; Zhang, Y.; Wu, X.; Zhu, C. and Gao, J. (2015). Atmospheric Emission Characteristics and Control Policies of Five Precedent-Controlled Toxic Heavy Metals from Anthropogenic Sources in China. *Environmental Science & Technology*, *49*, 1206-1214.

Chunhabundit, R. (2016). Cadmium Exposure and Potential Health Risk from Foods in Contaminated Area, Thailand. *Toxicological Research*, *32*, 65-72.

Das, P.; Sarma, K.P. and Kumar, M. (2015). Understanding of Chemical Speciation of Lead, Zinc and Copper in Vertical Profile of the Sediments of the Brahmaputra River, Assam, India. *International Journal of Environmental Sciences*, *12*.

Dhiman, A.; Ramanthan, A.L.; Macklin, M.; Yadav, S.; Kushwaha, S.; Mudbhatkal, A. and Senapathi, V. (2023). Heavy metal distribution in various environmental matrices and their risk assessment in Ganga River Basin, India. *Human and Ecological Risk Assessment: An International Journal*, *29*, 621-650.

Diamantini, E.; Lutz, S.R.; Mallucci, S.; Majone, B.; Merz, R. and Bellin, A. (2018). Driver detection of water quality trends in three large European river basins. *Science of The Total Environment*, *612*, 49-62.

Du, H. and Lu, X. (2022). Spatial distribution and source apportionment of heavy metal(loid)s in urban topsoil in Mianyang, Southwest China. *Scientific Reports*, *12*, 10407.

Duncan, D.B. (1955). Multiple range and multiple F tests. *Biometrics*, *11*, 1-42.

EBRD. (2018). *Kitchener Drain Depollution Project- Solid Waste*, Project ID: 29416.

Edgell, K. (1996). *US EPA Method 3050B: Acid digestion of sediments, sludges, and soils*. United States Environmental Protection Agency: Washington, DC.

El-Amier, Y.A.; Kotb, W.K.; Bonanomi, G.; Fakhry, H.; Marraiki, N.A. and Abd-ElGawad, A.M. (2021). Hydrochemical Assessment of the Irrigation Water Quality of the El-Salam Canal, Egypt. *Water*, *13*, 2428.

El-Amier, Y.A.; Bonanomi, G. and Abd-ElGawad, A.M. (2023). Pollution Risk Assessment of Heavy Metals along Kitchener Drain Sediment, Nile Delta. *Soil Systems*, *7*, 85.

El-Said Salem, Z.; Attiah, A.M. and Abu-Alam, T. (2024). Hydrochemical characterization and sustainability assessment of Ismailia canal water, Eastern Nile Delta, Egypt: implications for human health and environmental safety. *Frontiers in Environmental Science*, *12*.

EPA. (1992). *EPA Method 3005A: Acid digestion of waters for total recoverable or dissolved metals for analysis by FLAA or ICP spectroscopy*.

Farrag, M.M.S.; El-Geddawy, M.-A.M.A. and Ahmed, Z.S.A. (2022). More evidences for the nutritional quality and future exploitation of the invasive crayfish *Procambarus clarkii* (Girard, 1852) from the River Nile, Egypt. *Egyptian Journal of Aquatic Research*, *48*, 151-156.

Geriesh, M.; El-Rayes, A.; Gomaa, R.; Kaiser, M. and Mohamed, M. (2015). Geoenvironmental impact assessment of El-Salam Canal on the surrounding soil and groundwater flow regime, Northwestern Sinai, Egypt. *Catrina: The International Journal of Environmental Sciences*, *12*, 17-29.

Geriesh, M.H.; Balke, K.D. and El-Rayes, A.E. (2008). Problems of drinking water treatment along Ismailia Canal Province, Egypt. *Journal of Zhejiang University. Science. B*, *9*, 232-242.

Gerringa, L.J.A.; Alderkamp, A.-C.; van Dijken, G.; Laan, P.; Middag, R. and Arrigo, K.R. (2020). Dissolved Trace Metals in the Ross Sea. *Frontiers in Marine Science*, *7*.

Gupta, D.; Shukla, R. and Kumar Mishra, V. (2025). Heavy metal distribution, fractionation, metal pollution and environmental risk assessment in surface sediment of Narmada River, India. *International Journal of Environmental Analytical Chemistry*, *105*, 1881-1902.

Hacısalihoğlu, S. and Karaer, F. (2016). Relationships of Heavy Metals in Water and Surface Sediment with Different Chemical Fractions in Lake Uluabat, Turkey. *Polish Journal of Environmental Studies*, *25*.

Halim, M.A.; Rahman, M.M.; Mondal, D.; Megharaj, M. and Naidu, R. (2021). Bioaccumulation and Tolerance Indices of Cadmium in Wheat Plants Grown in Cadmium-Spiked Soil: Health Risk Assessment. *Frontiers in Environmental Science*, *9*.

Hamed, M.A.R. (2019). Characterization of surface water quality along Ismailia canal, nile river, Egypt. *Journal of Advanced Civil Engineering*, *2*, 01-14.

Harlıoğlu, M.M.; Köprücü, K.; Harlıoğlu, A.G.; Yılmaz, Ö.; Mişe Yonar, S.; Aydın, S. and Çakmak Duran, T. (2015). Effects of dietary n-3 polyunsaturated fatty acids on the nutritional quality of abdomen meat and hepatopancreas in a freshwater crayfish (*Astacus leptodactylus*). *Journal of Food Composition and Analysis*, *41*, 144-150.

Hussain, M.I.; Naeem, M.; Khan, Z.I.; Akhtar, S.; Nadeem, M.; Alnuwaiser, M.A.; Ahmad, K.; Vicente, O. and Yang, H.-H. (2022). Cadmium (Cd) and Copper (Cu) Exposure and Bioaccumulation Arrays in Farm Ruminants: Impact of Forage Ecotypes, Ecological Sites and Body Organs. *Sustainability,* *14*, 12595.

Ibironke, S.; Adepeju, A.; Otutu, O.; Oyedele, D. and Esan, Y. (2018). Nutritional evaluation and comparison study of seafoods such as fish and crayfish supplement dietary. *MOJ Food Processing & Technology*, *1*, 75-78.

Ibrahim, S.S.; Bakery, H.; El-Shawarby, R.; Abuo Salem, M. and Nabila, M. (2014). Incidence of some pollutants in ismailia canal and using different methods for removal. *Benha Veterinary Medical Journal*, *27*, 62-77.

Jibrin, B.; Jidauna, S.B. and Kefas, M. (2025). Species-Specific Bioaccumulation of Heavy Metals in *Oreochromis Niloticus*, *Synodontis Clarias* and *Clarias Gariepinus* from Kiri Reservoir, Nigeria. *British Journal of Multidisciplinary and Advanced Studies*, *6*, 1-11.

Jung, H.-B.; Yun, S.-T.; Mayer, B.; Kim, S.-O.; Park, S.-S. and Lee, P.-K. (2005). Transport and sediment–water partitioning of trace metals in acid mine drainage: an example from the abandoned Kwangyang Au–Ag mine area, South Korea. *Environmental Geology*, *48*, 437-449.

Khalifa, W. (2014). Simulation of water quality for the El-Salam canal in Egypt. *Water Pollution*, 27-37.

Khalifa, W.M. (2020). Evaluation of water quality parameters using numerical modeling approach for the El-Salam Canal in Egypt. *International Journal of Advanced and Applied Sciences*, *7*, 99-112.

Krishna Kamble, R. (2020). Source of groundwater iron and manganese in Chandrapur district, central India. *The Holistic Approach to Environment*, *10*, 53-72.

Kuklina, I.; Kouba, A. and Kozák, P. (2013). Real-time monitoring of water quality using fish and crayfish as bio-indicators: a review. *Environmental Monitoring and Assessment*, *185*, 5043-5053.

Kumari, D. and Paul, D.K. (2020). Assessing the role of bioindicators in freshwater ecosystem. *Journal of Interdisciplinary Cycle Research*, *12*, 17.

Kutlu, B.; Çevik, F. and Çetindağ, S. (2025). Assessments of heavy metal contaminations of surface water and sediment of Pülümür Stream (Türkiye). *Environmental Forensics*, *26*, 107-121.

Labuschagne, M. (2019). *Validation of artificial mussels as indicators of platinum group element exposure in the Hex River System*. North-West University (South Africa), Potchefstroom Campus.

Lee, J.W.; Jo, A.H.; Kang, Y.J.; Lee, D.; Choi, C.Y.; Kang, J.C. and Kim, J.H. (2024). Review of Cadmium Bioaccumulation in Fish Exposed to Cadmium. *Toxics*, *13*.

Li, S.; Chen, J.; Zhang, X.; Zhang, J.; Xu, Y. and Xu, Y. (2025). Heavy metal distribution and ecological risk in surface sediments of the Bohai Sea. *PLOS ONE*, *20*, e0326701.

Lim, W.Y.; Aris, A.Z. and Zakaria, M.P. (2012). Spatial variability of metals in surface water and sediment in the langat river and geochemical factors that influence their water-sediment interactions. *The Scientific World Journal*, *2012*, 652150.

Liu, Y.; Chen, Q.; Li, Y.; Bi, L.; Jin, L. and Peng, R. (2022). Toxic Effects of Cadmium on Fish. *Toxics*, *10*.

M'Kandawire, E.; Mierek-Adamska, A.; Stürzenbaum, S.R.; Choongo, K.; Yabe, J.; Mwase, M.; Saasa, N. and Blindauer, C.A. (2017). Metallothionein from Wild Populations of the African Catfish *Clarias gariepinus*: From Sequence, Protein Expression and Metal Binding Properties to Transcriptional Biomarker of Metal Pollution. *International Journal of Molecular Sciences*, *18*.

Mamun, S.; Nahar, N.; Ata Ullah, M.; Abduz Zaher, M. and Paul, T. (2024). Assessment of Heavy Metal Contamination and Potential Health Risk of Selected Fish Species in Dhaka District. *Bioresearch Communications*, *10*, 1524-1531.

Mathers, K.L.; Chadd, R.P.; Extence, C.A.; Rice, S.P. and Wood, P.J. (2016). The implications of an invasive species on the reliability of macroinvertebrate biomonitoring tools used in freshwater ecological assessments. *Ecological Indicators*, *63*, 23-28.

Mazza, G.; Tricarico, E.; Genovesi, P. and Gherardi, F. (2014). Biological invaders are threats to human health: an overview. *Ethology Ecology & Evolution*, *26*, 112-129.

Melake, B.A.; Endalew, S.M.; Alamirew, T.S. and Temesegen, L.M. (2023). Bioaccumulation and Biota-Sediment Accumulation Factor of Metals and Metalloids in Edible Fish: A Systematic Review in Ethiopian Surface Waters. *Environmental Health Insights*, *17*, 11786302231159349.

Metwally, A.A.; Khalafallah, M.M. and Dawood, M.A.O. (2023). Water quality, human health risk, and pesticides accumulation in African catfish and Nile tilapia from the Kitchener Drain-Egypt. *Scientific Reports*, *13*, 18482.

Min, E.Y.; Ahn, T.Y. and Kang, J.-C. (2016). Bioaccumulation, alterations of metallothionein, and antioxidant enzymes in the mullet *Mugil cephalus* exposed to hexavalent chromium. *Fisheries and Aquatic Sciences*, *19*, 19.

Mishra, B.; Gautam, G.J.; Chaturvedi, R.K.; Ansari, N.G. and Mishra, V.N. (2024). Ecological and Health Risk Assessment of Heavy Metals Bioaccumulation in Ganges Fish Near Varanasi, India. *Biological Trace Element Research*, *202*, 4751-4766.

Mona, M.M.; Younis, M.L. and Atlam, A.I. (2023). Evaluation of freshwater heavy metals accumulation effect on oxidative stress, Metallothionein biosynthesis and histopathology of *Procambarus clarkii* (Girard,1985) collected from three locations in the Delta region, Egypt. *BMC Zoology*, *8*, 21.

Nurdini, J.A.; Hidayati, D.R.; Cahya, I.; Noviani, A. and Ridyawati, I.W. (2024). Distribution of Pb and Fe heavy metal contamination in sea water and sediment in Bangkalan Madura Sea Waters. *E3S Web of Conferences*, *499*, 01025.

Páez-Osuna, F.; Bergés-Tiznado, M.E.; Valencia-Castañeda, G.; Fregoso-López, M.G.; León-Cañedo, J.A.; Fierro-Sañudo, J.F. and Ramírez-Rochín, J. (2023). Metal(loid)s (As, Cd, Cu, and Zn) in three fish species from a dam after a mine-tailing spill: differential bioaccumulation and potential health risk. *Environmental Geochemistry and Health*, *45*, 4533-4548.

Pastor-Arbulú, P. and Rodríguez-Delfín, A. (2025). Seaweed-based biostimulant alleviates cadmium-induced physiological stress in tomato (*Solanum lycopersicum* L.). *BMC Plant Biology*, *25*, 1016.

Peana, M.; Pelucelli, A.; Chasapis, C.T.; Perlepes, S.P.; Bekiari, V.; Medici, S. and Zoroddu, M.A. (2022). Biological Effects of Human Exposure to Environmental Cadmium. *Biomolecules*, *13*.

Peters, A.; Merrington, G. and Middleton, E. (2024). How important is it to update the existing environmental quality standard for nickel? An example based on the UK. *Environmental Science: Advances*, *3*, 1139-1152.

Ramadan, E.M.; Abdelwahab, H.F.; Vranayova, Z.; Zelenakova, M. and Negm, A.M. (2021). Optimization-Based Proposed Solution for Water Shortage Problems: A Case Study in the Ismailia Canal, East Nile Delta, Egypt. *Water*, *13*, 2481.

Remeteiová, D.; Ružičková, S.; Mičková, V.; Laubertová, M. and Slezáková, R. (2020). Evaluation of US EPA method 3052 microwave acid digestion for quantification of majority metals in waste printed circuit boards. *Metals*, *10*, 1511.

Rendina, A.; Cabo, L.d.; Arreghini, S.; Bargiela, M. and Fabrizio de Iorio, A. (2001). Geochemical distribution and mobility factors of Zn and Cu in sediments of the Reconquista River, Argentina. *Revista Internacional de Contaminación Ambiental*, *17*, 187-192.

Salauddin, A. and Sandesh, C.J. (2023). Heavy metal pollution of soil and crops in rural Gujarat, next to an industrial area: a correlation study. *Nature Environment and Pollution Technology*, *22*, 691-698.

Sankhla, M.S.; Kumari, M.; Nandan, M.; Kumar, R. and Agrawal, P. (2016). Heavy metals contamination in water and their hazardous effect on human health-a review. *International Journal of Current Microbiology and Applied Sciences*, *5*, 759-766.

Senarathne, P. and Pathiratne, K.A.S. (2010). Accumulation of heavy metals in a food fish, *Mystus gulio* inhabiting Bolgoda Lake, Sri Lanka. *Sri Lanka Journal of Aquatic Sciences*.

Stanek, M.; Dąbrowski, J.; D³ugosz, J. and Janicki, B. (2014). Impact of the Anthropogenisation on the Metal Bioaccumulation and Distribution in the Spiny-Cheek Crayfish (*Orconectes limosus* Raf.) from Lake Gop³o, Poland. *International Journal of Environmental Research*, *8*, 1315-1322.

Sumudumali, R. and Jayawardana, J. (2021). A review of biological monitoring of aquatic ecosystems approaches: with special reference to macroinvertebrates and pesticide pollution. *Environmental Management*, *67*, 263-276.

The Risk Assessment Information System. (2019). University of Tennessee. Available from: https://rais.ornl.gov/index.html.

Thiep, V.V.; Tran, T.Y. and Hoang, A.V. (2020). Assessment of heavy metals content and consumer health risk to *Siganus fuscescens* (Houttuyn, 1782) from Quang Binh province. *The Journal of Agriculture and Development*, *19*, 46-54.

Thomann, R.V.; Mahony, J.D. and Mueller, R. (1995). Steady-state model of biota sediment accumulation factor for metals in two marine bivalves. *Environmental Toxicology and Chemistry*, *14*, 1989-1998.

UNEP/RAMOGE. (1999). *Manual on the biomarkers recommended for the MED POL biomonitoring programme*. UNEP: Athens, Greece.

Vallese, F.D.; Stupniki, S.; Trillini, M.; Belén, F.; Di Nezio, M.S.; Juan, A. and Pistonesi, M.F. (2025). Bioaccumulation Study of Cadmium and Lead in *Cyprinus carpio* from the Colorado River, Using Automated Electrochemical Detection. *Journal of Analytical Methods in Chemistry*, *17*, 77.

Velusamy, S.; Roy, A.; Sundaram, S. and Mallick, T.K. (2022). Concern for heavy metal ion water pollution: Their strategic detection and removal opportunities. In: *Contaminants of Emerging Concerns and Reigning Removal Technologies*. CRC Press, pp. 257-284.

Viarengo, A.; Ponzano, E.; Dondero, F. and Fabbri, R. (1997). A simple spectrophotometric method for metallothionein evaluation in marine organisms: an application to Mediterranean and Antarctic molluscs. *Marine Environmental Research*, *44*, 69-84.

Wang, W.-C.; Mao, H.; Ma, D.-D. and Yang, W.-X. (2014). Characteristics, functions, and applications of metallothionein in aquatic vertebrates. *Frontiers in Marine Science*, *1*.

Younis, A.; Elnaggar, D.; Mohamedein, L. and Kolesnikov, A. (2023). Assessment of heavy metal distribution, contamination, and ecological risk in mangrove sediments of the Nabq Protectorate, Gulf of Aqaba. *Egyptian Journal of Aquatic Biology and Fisheries*, *27*, 1299-1320.

Zahedi, M.M. (2018). Biota-sediment accumulation factor and concentration of heavy metals (Hg, Cd, As, Ni, Pb and Cu) in sediments and tissues of *Chiton lamyi* (Mollusca: Polyplacophora: Chitonidae) in Chabahar Bay, Iran. *Iranian Journal of Fisheries Sciences*, *3*.

Zaitsev, G.A.; Dubrovina, O.A. and Shainurov, R.I. (2020). Iron and manganese migration in "soil–plant" system in Scots pine stands in conditions of contamination by the steel plant's emissions. *Scientific Reports*, *10*, 11025.

Zhang, Y.; Yang, B.; Yang, L.; Jiang, S.; Lu, J. and Lin, L. (2023). Comparison of the nutritional qualities of the pond, rice-field and wild crayfish (*Procambarus clarkii*) meat. *Food Chemistry Advances*, *2*, 100272.

Zorita, I.; Strogyloudi, E.; Buxens, A.; Mazón, L.I.; Papathanassiou, E.; Soto, M. and Cajaraville, M.P. (2005). Application of two SH-based methods for metallothionein determination in mussels and intercalibration of the spectrophotometric method: laboratory and field studies in the Mediterranean Sea. *Biomarkers*, *10*, 342-359.

Appendix

List of Tables

Table 2. Heavy metal concentrations across environmental matrices and geographic locations

Location	Matrix	Cd (mg/kg)	Cu (mg/kg)	Fe (mg/kg)	Pb (mg/kg)	Mn (mg/kg)	Zn (mg/kg)	Ni (mg/kg)
Mostorod	**Crayfish**	**0.080±0.006^{c}**	**0.012±0.001^{b}**	**0.150±0.004^{b}**	**0.002±0.000**	**0.001±0.000**	**0.367±0.033^{c}**	ND
	Water	**0.002±0.000**	**0.016±0.001**	**0.021±0.001^{c}**	**0.007±0.000**	**0.037±0.001^{a}**	**0.030±0.006^{c}**	ND
	Sediment	**0.003±0.000**	**0.813±0.009^{a}**	**0.150±0.006^{a}**	**0.007±0.000**	**0.019±0.001^{a}**	**1.200±0.058^{a}**	ND
El-Sharqia	**Crayfish**	**0.120±0.002^{b}**	**0.015±0.002^{a}**	**0.140±0.003^{b}**	**0.002±0.000**	**0.001±0.000**	**0.523±0.009^{b}**	ND
	Water	**0.002±0.000**	**0.017±0.001**	**0.046±0.001^{b}**	**0.007±0.000**	**0.011±0.001^{b}**	**0.072±0.006^{a}**	ND
	Sediment	**0.002±0.000**	**0.610±0.007^{b}**	**0.130±0.003^{b}**	**0.005±0.000**	**0.015±0.001^{b}**	**1.000±0.053^{b}**	ND
Kafr El-Sheikh	**Crayfish**	**0.410±0.006^{a}**	**0.015±0.001^{a}**	**0.280±0.006^{a}**	**0.002±0.000**	**0.003±0.000**	**0.620±0.006^{a}**	ND
	Water	**0.002±0.000**	**0.018±0.001**	**0.050±0.001^{a}**	**0.007±0.000**	**0.038±0.001^{a}**	**0.053±0.005^{b}**	ND
	Sediment	**0.002±0.000**	**0.500±0.006^{c}**	**0.120±0.004^{b}**	**0.004±0.000**	**0.011±0.001^{c}**	**0.800±0.050^{c}**	ND

Note: Values represent mean ± standard error. Letters (a, b, c) indicate significant differences within each matrix type (Duncan's test, $P < 0.05$). ND = Not Detected.

Table 3. Bioaccumulation factor (BAF) between crayfish and water at different sites

Area	Cd (mg/kg)	Cu (mg/kg)	Fe (mg/kg)	Mn (mg/kg)	Zn (mg/kg)
Mostorod	**40.00±2.89^{c}**	**0.73±0.01^{b}**	**7.15±0.24^{a}**	**0.03±0.00^{b}**	**13.61±3.61**
El-Sharqia	**60.00±3.05^{b}**	**0.88±0.01^{a}**	**3.04±0.11^{c}**	**0.09±0.01^{a}**	**7.35±0.68**
Kafr El-Sheikh	**205.00±2.89^{a}**	**0.82±0.03^{a}**	**5.60±0.10^{b}**	**0.08±0.01^{a}**	**11.99±1.22**

Note: Values represent mean ± standard error. Letters (a, b, c) indicate significant differences within each matrix type (Duncan's test, $P < 0.05$).

Table 4. Biota–sediment accumulation factor (BSAF) between crayfish and sediment at different sites

Area	Cd (mg/kg)	Cu (mg/kg)	Fe (mg/kg)	Mn (mg/kg)	Zn (mg/kg)
Mostorod	**26.67±1.93^{c}**	**0.01±0.00^{b}**	**1.00±0.01^{b}**	**0.05±0.00^{b}**	**0.31±0.03^{c}**
El-Sharqia	**60.00±0.00^{b}**	**0.02±0.00^{a}**	**1.08±0.01^{b}**	**0.07±0.00^{b}**	**0.53±0.03^{b}**
Kafr El-Sheikh	**205.00±2.89^{a}**	**0.03±0.00^{a}**	**2.34±0.06^{a}**	**0.27±0.01^{a}**	**0.78±0.06^{a}**

Note: Values represent mean ± standard error. Letters (a, b, c) indicate significant differences within each matrix type (Duncan's test, $P < 0.05$).

Table 5. People health risk parameters in crayfish from three areas in Egyptian Delta

Elements	**Cd (mg/kg)**			**Cu (mg/kg)**			**Fe (mg/kg)**			**Zn (mg/kg)**			
Site	EDI	THQ	RFD	EDI	THQ	RFD	EDI	THQ	RFD	EDI	THQ	RFD	HI
Mostorod	0.006	0.009	0.004	0.001	0.0001	0.04	0.011	0.0002	0.7	0.028	0.002	0.3	0.011
El-Sharqia	0.009	0.021		0.001	0.0000		0.011	0.0002		0.040	0.005		0.026
Kafr El-Sheikh	0.031	0.241		0.001	0.0000		0.021	0.0006		0.047	0.007		0.249

Note: Values represent mean ± standard error. Letters (a, b, c) indicate significant differences within each matrix type (Duncan's test, $P < 0.05$).

List of Figs.

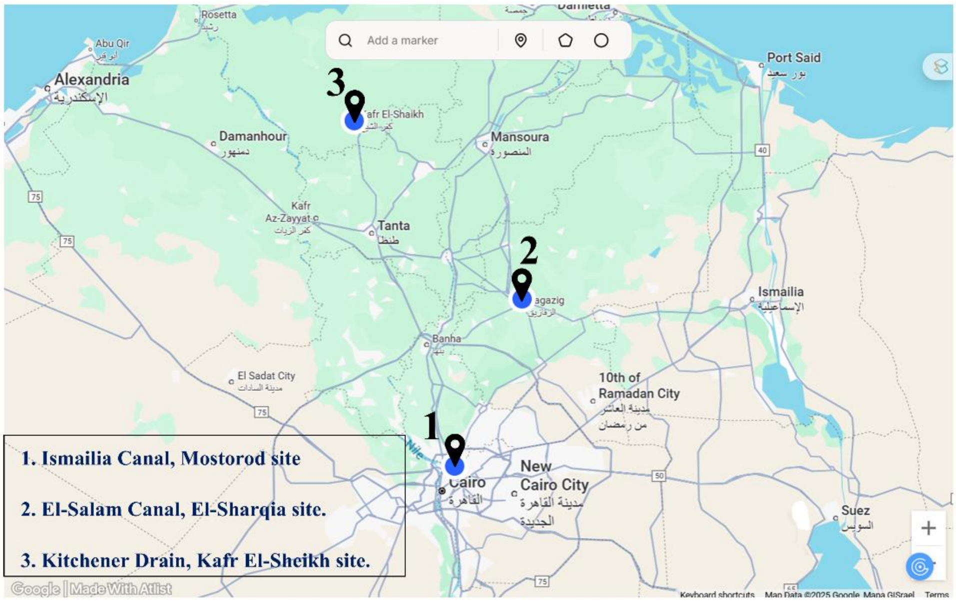

Fig. 1. Locations of collected samples

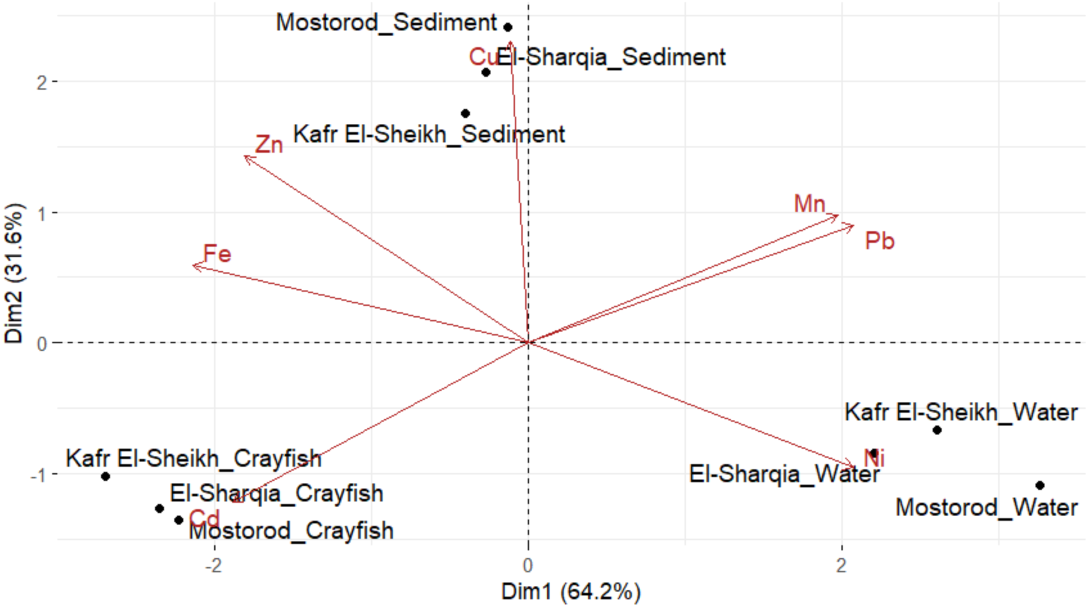

Fig. 2. PCA Biplot of heavy metal concentrations across environmental matrices from three Egyptian locations

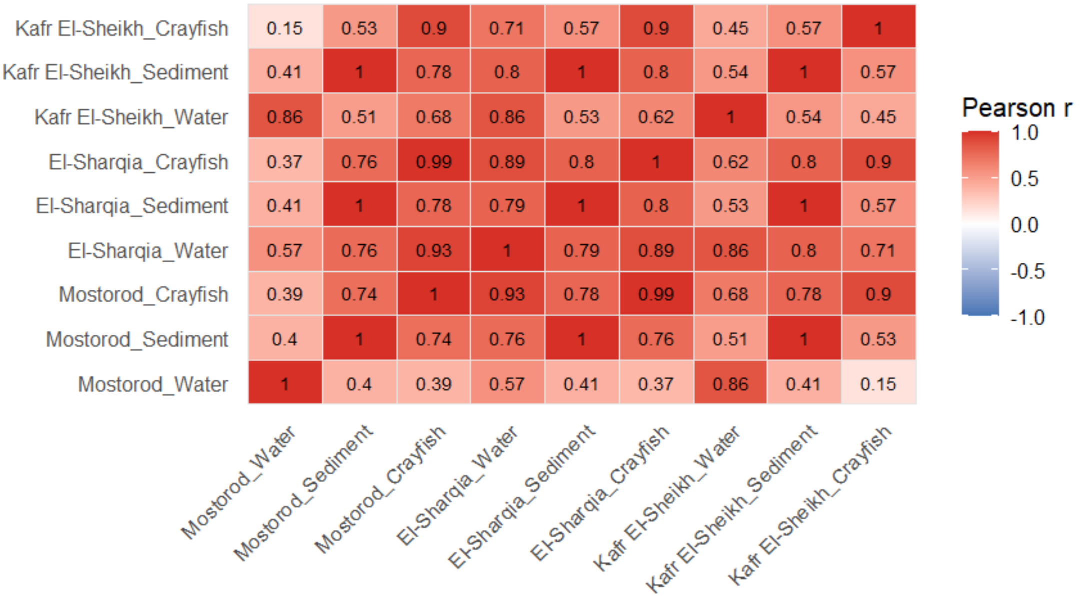

	Mostorod_Water	Mostorod_Sediment	Mostorod_Crayfish	El-Sharqia_Water	El-Sharqia_Sediment	El-Sharqia_Crayfish	Kafr El-Sheikh_Water	Kafr El-Sheikh_Sediment	Kafr El-Sheikh_Crayfish
Kafr El-Sheikh_Crayfish	0.15	0.53	0.9	0.71	0.57	0.9	0.45	0.57	1
Kafr El-Sheikh_Sediment	0.41	1	0.78	0.8	1	0.8	0.54	1	0.57
Kafr El-Sheikh_Water	0.86	0.51	0.68	0.86	0.53	0.62	1	0.54	0.45
El-Sharqia_Crayfish	0.37	0.76	0.99	0.89	0.8	1	0.62	0.8	0.9
El-Sharqia_Sediment	0.41	1	0.78	0.79	1	0.8	0.53	1	0.57
El-Sharqia_Water	0.57	0.76	0.93	1	0.79	0.89	0.86	0.8	0.71
Mostorod_Crayfish	0.39	0.74	1	0.93	0.78	0.99	0.68	0.78	0.9
Mostorod_Sediment	0.4	1	0.74	0.76	1	0.76	0.51	1	0.53
Mostorod_Water	1	0.4	0.39	0.57	0.41	0.37	0.86	0.41	0.15

Fig. 3. Correlation heat-map of heavy metals by site and sample type

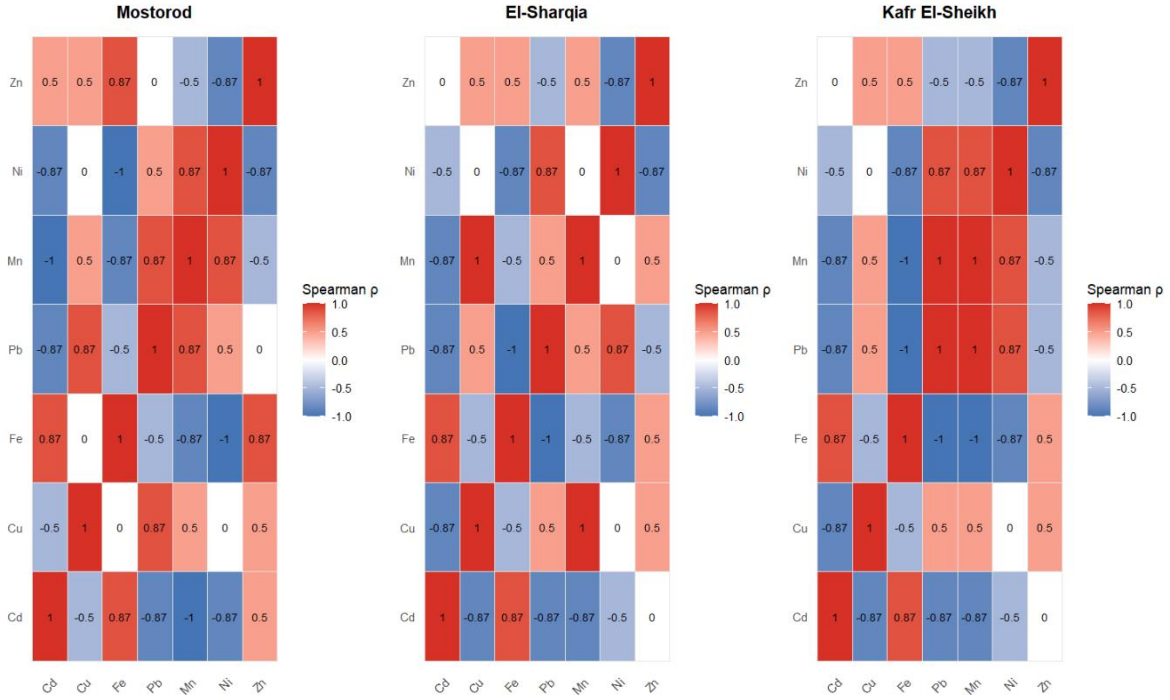

Mostorod

	Cd	Cu	Fe	Pb	Mn	Ni	Zn
Zn	0.5	0.5	0.87	0	-0.5	-0.87	1
Ni	-0.87	0	-1	0.5	0.87	1	-0.87
Mn	-1	0.5	-0.87	0.87	1	0.87	-0.5
Pb	-0.87	0.87	-0.5	1	0.87	0.5	0
Fe	0.87	0	1	-0.5	-0.87	-1	0.87
Cu	-0.5	1	0	0.87	0.5	0	0.5
Cd	1	-0.5	0.87	-0.87	-1	-0.87	0.5

El-Sharqia

	Cd	Cu	Fe	Pb	Mn	Ni	Zn
Zn	0	0.5	0.5	-0.5	0.5	-0.87	1
Ni	-0.5	0	-0.87	0.87	0	1	-0.87
Mn	-0.87	1	-0.5	0.5	1	0	0.5
Pb	-0.87	0.5	-1	1	0.5	0.87	-0.5
Fe	0.87	-0.5	1	-1	-0.5	-0.87	0.5
Cu	-0.87	1	-0.5	0.5	1	0	0.5
Cd	1	-0.87	0.87	-0.87	-0.87	-0.5	0

Kafr El-Sheikh

	Cd	Cu	Fe	Pb	Mn	Ni	Zn
Zn	0	0.5	0.5	-0.5	-0.5	-0.87	1
Ni	-0.5	0	-0.87	0.87	0.87	1	-0.87
Mn	-0.87	0.5	-1	1	1	0.87	-0.5
Pb	-0.87	0.5	-1	1	1	0.87	-0.5
Fe	0.87	-0.5	1	-1	-1	-0.87	0.5
Cu	-0.87	1	-0.5	0.5	0.5	0	0.5
Cd	1	-0.87	0.87	-0.87	-0.87	-0.5	0

Fig.4. Spearman rank correlation coefficients between heavy metal concentrations at three sampling sites

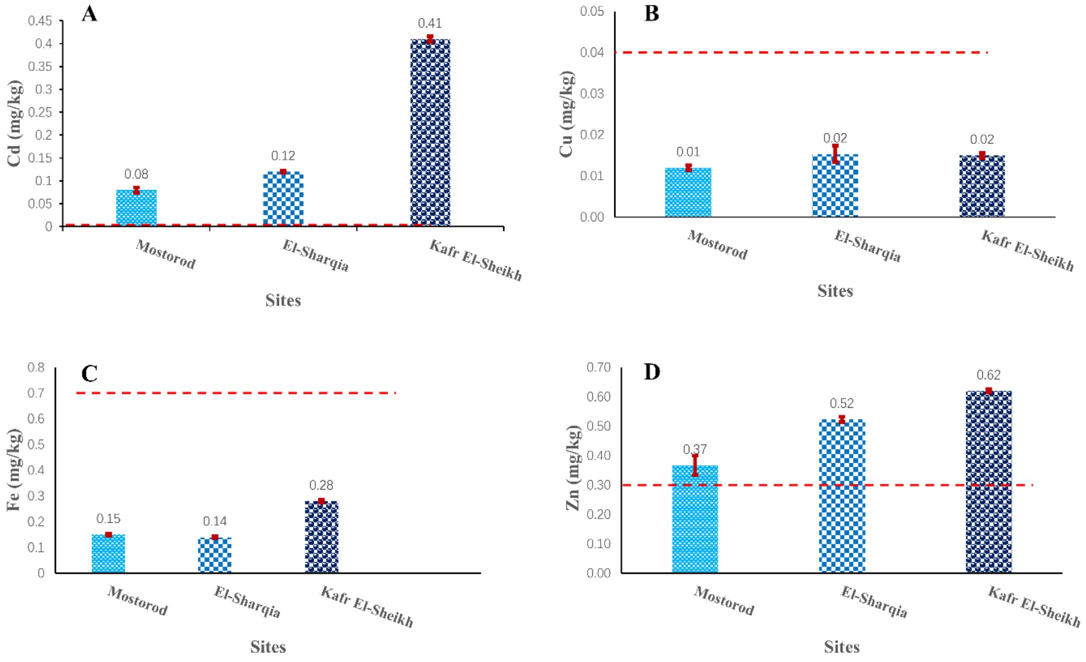

Fig. 5. Heavy metals (mg/kg) in crayfish collected from the three sites of the Egyptian Delta. Each value is the mean for three replicates. The target line is a standard of heavy metals according to (The Risk Assessment Information System, 2019). ^{A} Cd; ^{B} Cu; ^{C} Fe; and ^{D} Zn

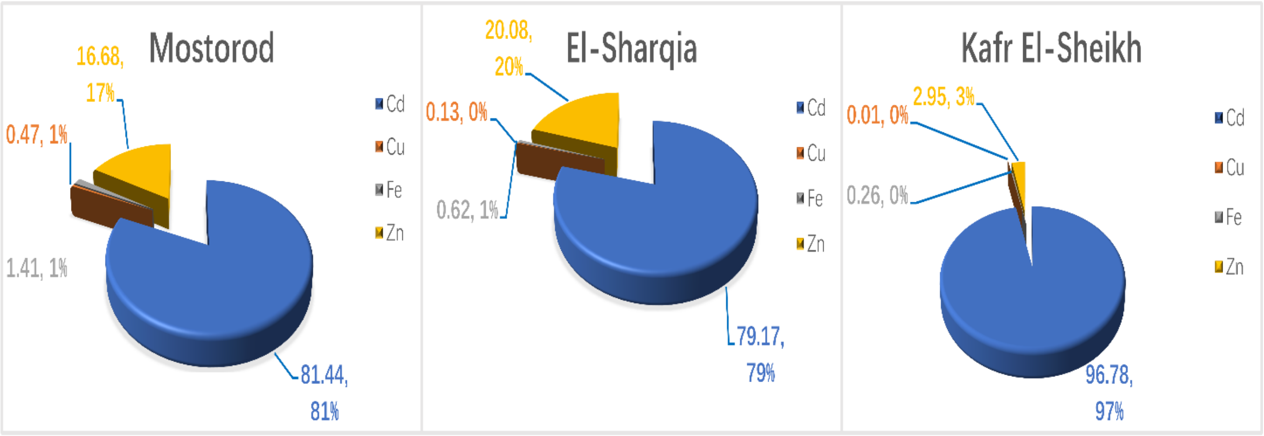

Fig. 6. Average percentage contribution of Cd, Cu, Fe and Zn to the hazard index at the three sites of this study

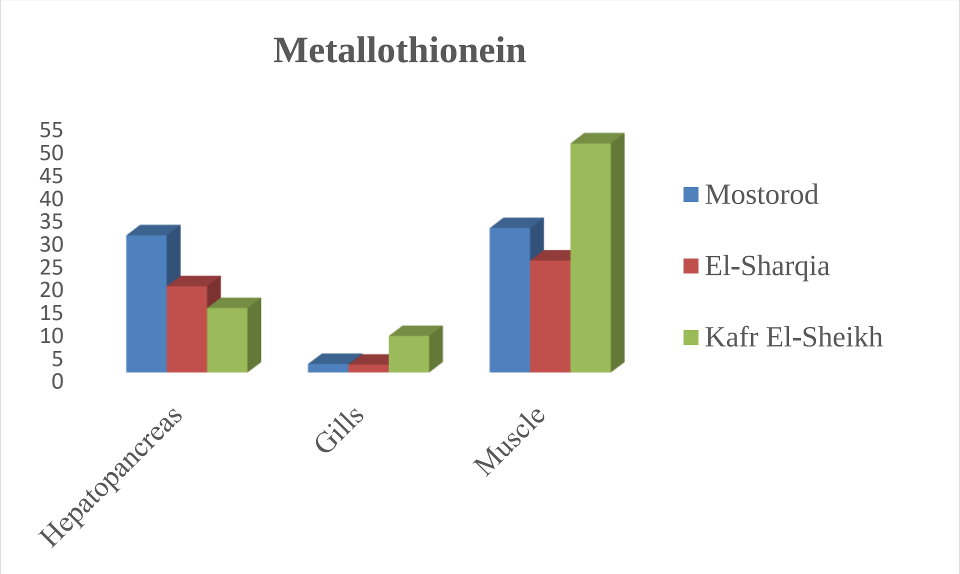

Fig. 7. Metallothionein protein concentration in organs of crayfish